

“© 2015 IEEE. Personal use of this material is permitted. Permission from IEEE must be obtained for all other uses, in any current or future media, including reprinting/republishing this material for advertising or promotional purposes, creating new collective works, for resale or redistribution to servers or lists, or reuse of any copyrighted component of this work in other works.”

# Incumbent User Active Area Detection for Licensed Shared Access

B. A. Jayawickrama, E. Dutkiewicz  
Macquarie University, Australia  
Email: {beeshanga.abewardana,  
eryk.dutkiewicz}@mq.edu.au

Markus Mueck  
Intel Mobile Communications, Germany  
Email: markus.dominik.mueck@intel.com

**Abstract**—Licensed Shared Access is a European standardisation effort which promotes repository based quasi-static hierarchical spectrum sharing. In this scheme the sharing time base is in the order of months if not years. For widespread use of Licensed Shared Access, shrinking the sharing time base is crucial. In this paper we propose a scheme to reduce the sharing time base to seconds or minutes scale. We present a new technique named lightweight Radio Environment Map based on a Kalman Filter derived from geo-location aware spectrum measurements, which can be run at the shared access licensee end. Our objective is to determine the active area of a static or slowly moving incumbent. We consider a challenging scenario where a large fraction of measurements is missing and the available measurements are highly distorted. Performance of our incumbent active area detection approach is evaluated by simulating a low power incumbent in an urban cellular environment. Simulation results show a substantial improvement of missed detection area in comparison to the counterpart that does not use our lightweight Radio Environment Map.

**Index Terms**—Licensed Shared Access, Kalman Filter, Maximum Likelihood Estimation

## I. INTRODUCTION

Over the last few decades, cellular technology has come a long way considering the enhancement in throughput and Quality of Service (QoS). Although the engineered solutions have well defined bounds, the mobile user traffic is limited only by their imagination. In meeting the demand of future cellular, more spectrum resources under 6 GHz need to be allowed for use in cellular applications. To promote spectrum sharing as a potential solution the European Telecommunications Standards Institute Reconfigurable Radio Systems (ETSI RRS) Technical Standardisation Committee has proposed a new approach named Licensed Shared Access (LSA) [1].

In LSA architecture, the incumbent and a LSA licensee come to a mutual agreement on a sharing policy. LSA licensee is typically a cellular operator. To allow better quality of service the sharing time base is currently in the order of years. However finding suitable bands for this quasi-static sharing scheme where the incumbent agrees to cooperate for a long duration is not trivial, which limits widespread use of LSA. By shrinking the sharing time base finding suitable bands will turn out less challenging.

To strike a balance between two extremes, we propose a framework that shrinks the sharing time base of LSA down to a seconds/minutes range only. This paper is based on our previous work on *Radio Environment Maps* (REM)

[2], [3], a technique of generating a heatmap which shows how the *Received Signal Strength* (RSS) varies over space. Therein we considered the scenario where both location and transmit power of incumbents are not known due to absence of a LSA repository. We then found an estimation to the incumbent active area primarily using  $\ell_1$ -norm minimisation theory. However, the work did not exploit the concurrent implementation of LSA architecture. Also in [4], the authors use a well known spatial interpolation technique called Kriging to construct a REM. In [5] authors derive a Bayesian Kriging interpolation model. In a large cellular network Kriging related techniques tend to fall into offline processing category, due to the computational complexity.

In the interest of keeping communication and computation overhead minimal, we propose *light-REM*, a novel approach to constructing REMs. Our scheme significantly differs from the traditional REM approach found in literature as we exploit the location information of a static/slowly moving incumbent provided by the LSA repository. This paper casts light-REM construction as a *Kalman Filter* (KF) problem by exploiting long coherence time of large scale fading characteristics of wireless channels. This is achieved by *User Equipment* (UE) exchanging training symbols. This allows the base station to learn and track wireless channels of interest, further illustrated in Section II. UE collect geo-location aware RSS measurements of the incumbent signal. By putting together incumbent location information provided by LSA along with UE measurements we take the maximum likelihood estimation for the incumbent transmit power, which is directly related to the incumbent active area. Further, we consider a challenging scenario where the majority of measurements are missing and/or heavily distorted. Under these circumstances we illustrate how our light-REM based maximum likelihood approach outperforms the counterpart that doesn't use a light-REM.

In Section II we introduce our system model and illustrate how LSA architecture is extended in our work. Problem formulation and our proposed solution based on light-REM and maximum likelihood estimation of incumbent active area are presented in Section III, IV and V. Simulation results and analysis can be found in Section VI.

## II. SYSTEM MODEL

We consider the scenario where a static or slowly moving incumbent is present in an urban microcellular environment.

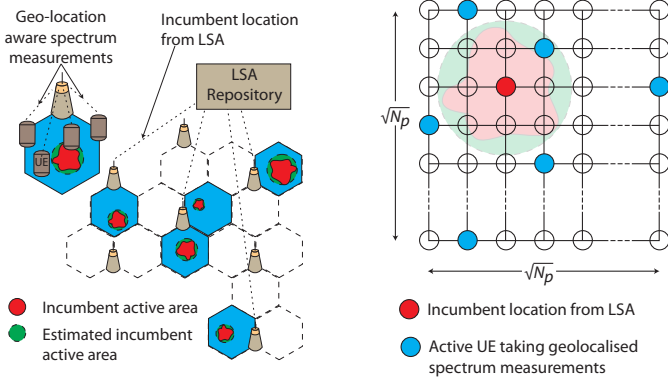


Fig. 1. System model: the LSA repository informs the LSA licensee base stations regarding the location of potentially active incumbents. Base stations use geo-location aware spectrum measurements from UE to estimate the incumbent active geographical area.

LSA licensee is an operator that intends allowing its users to exploit LSA spectrum for localised spectrum usage scenarios such as femtocells, peer-to-peer applications, etc. In our system model the LSA repository contains the frequency and location information of this static or slowly moving incumbent. We assume a sharing time base is in the order of seconds if not minutes. LSA repository is however unable to provide information on whether the incumbent is active at any given point and if so the geographical area in which the spectrum needs to be made available for incumbent use. Architecture of the system is shown in Fig. 1.

In our work we define light-REM as a heatmap in  $\mathbb{R}^3$  showing power gains of channels from the incumbent location to other points in space. This paper demonstrates how a light-REM helps an operator to detect the incumbent active area in space. To reduce the complexity of the problem we consider discrete space composed of a grid structure as shown in Fig. 1. The incumbent and UE are assumed to be on grid. The error caused by considering discrete space is captured by a Gaussian process as illustrated in Section III.

UE are uniformly distributed where the probability of a UE actively participating in light-REM construction at any grid point is the same at all points. To reduce the power consumption of UE, their duties are limited to exchanging training symbols and performing geo-location aware RSS measurements only. Measurement results are forwarded to the base station which constructs a light-REM to determine the contour of geographical area where LSA spectrum is available. For this exchange the operator uses a dedicated common control channel from its own licenced bands.

### III. PROBLEM FORMULATION

In this section we formulate light-REM construction as a KF problem. Consider a discrete space composed of  $N_p$  grid points,  $N_s$  active UE performing spectrum measurements and one local incumbent. The probability of a UE actively engaging in light-REM construction at any given point is  $q$ . Suppose the incumbent is present at  $j$ th grid point, the received

signal at all  $N_p$  grid points at time  $t$  can be written as,

$$\mathbf{r} = \mathbf{H}s + \mathbf{n} \quad (1)$$

where  $\mathbf{H} = (h_{1j}, h_{2j}, \dots, h_{N_p j})^T$ ,  $h_{ij}$  is the complex coefficient of channel from  $j$  to  $i$ . Also,  $s$  is the transmitted signal of the incumbent and  $\mathbf{n}$  is a  $N_p \times 1$  AWGN vector. On a square grid layout the  $j$ th reference point can be mapped to (row, column) coordinates as:  $j \rightarrow (\lceil j/\sqrt{N_p} \rceil, j - \sqrt{N_p}(\lceil j/\sqrt{N_p} \rceil - 1))$ . Further we assume frequency-flat fading of the channel.

We calculate the Received Signal Strength (RSS) at  $N_p$  grid points as follows,

$$\mathbf{Pr} = \mathbf{E}[\mathbf{r} \circ \mathbf{r}^*] \quad (2)$$

$$= \mathbf{E}[(\mathbf{H}s + \mathbf{n}) \circ (\mathbf{H}s + \mathbf{n})^*] \quad (3)$$

where  $\circ$  is the Hadamard product. We also assume that noise is spatio-temporally white and independent of transmitted signal. Therefore we can rewrite (3) as follows,

$$\mathbf{Pr} = \mathbf{E}[(\mathbf{H}s) \circ (\mathbf{H}s)^*] + \mathbf{E}[\mathbf{n} \circ \mathbf{n}^*] \quad (4)$$

$$= \mathbf{\Psi}Pt + \sigma_n^2 \mathbf{1} \quad (5)$$

where  $\mathbf{\Psi}$  is the  $N_p \times 1$  channel gain vector given by  $[\mathbf{\Psi}]_i = \mathbf{E}[|h_{ij}|^2]$ ,  $Pt$  is the transmit power of the incumbent given by  $Pt = \mathbf{E}[|s|^2]$ ,  $\sigma_n^2$  is the variance of AWGN and  $\mathbf{1}$  is a vector of ones. We consider that only  $N_s$  receivers are performing spectrum measurements at any given time. Hence, the noisy spectrum measurement vector  $\mathbf{Ps}$  can be written as,

$$\mathbf{Ps} = \tilde{\mathbf{\Psi}}Pt + \sigma_n^2 \mathbf{1} + \boldsymbol{\eta} \quad (6)$$

where  $\tilde{\mathbf{\Psi}} = \mathbf{\Phi}\mathbf{\Psi}$ ,  $\mathbf{\Phi}$  is the  $N_s \times N_p$  matrix representing the geolocation of spectrum sensing UE as follows,

$$[\mathbf{\Phi}]_{kj} = \begin{cases} 1 & \text{if } k\text{th active UE is at } j\text{th reference point} \\ 0 & \text{otherwise} \end{cases} \quad (7)$$

In a practical implementation of our system errors may occur in measuring RSS, determining geo-location and approximating the location to the nearest grid point in discrete space. To capture such errors we add the  $N_s \times 1$  Gaussian noise vector  $\boldsymbol{\eta}$  in (6).

Hence, our problem can be stated as finding  $Pt$  in (6) based on the geo-localised RSS measurements  $\mathbf{Ps}$ . Our approach is two fold, we first construct a light-REM (i.e. estimate  $\mathbf{\Psi}$ ) using a KF as shown in Section IV. Then we take the maximum likelihood estimation approach to find  $Pt$  as shown in Section V. In the interest of keeping the computational complexity and traffic overhead minimal, the transmit power  $Pt$  is directly related to the incumbent active area using a pathloss model, as further illustrated in Section V.

### IV. KALMAN FILTER FOR LIGHT-REM CONSTRUCTION AND TRACKING

In this section we cast the light-REM construction as a discrete time KF problem. Consider the channel gains vector given by  $\mathbf{\Psi}$  which can be modelled as,

$$[\mathbf{\Psi}]_i = \mathbf{E}[|h_{ij}|^2] = \mathbf{E}[F_{ij}G_{ij}L_{ij}] \quad (8)$$

where  $F_{ij}$  captures the fast fading due to a multipath environment,  $G_{ij}$  models the shadow fading due to blockage and the pathloss is modelled using  $L_{ij}$ . To facilitate LSA in a seconds/minutes sharing time scale, the expectation operator refers to the time average taken over a short period such that it eliminates the impact of multipath fading, while large scale fading and path loss can be considered quasi-static. As the environmental changes do not occur rapidly, the coherence time of the large scale fading is substantially large and it is expected to spread over many measurement iterations depending on the application environment.

Therefore we can write,

$$[\Psi]_i = E[F]G_{ij}L_{ij} \quad (9)$$

Hence the channel estimation problem comes down to determining and tracking changes to  $G_{ij}L_{ij}$ . For this purpose, UE at  $j$ th grid point transmits a sequence of training symbols which is used by the UE at  $i$ th grid point to estimate  $[\Psi]_i$ . We run a discrete time KF that exploits the substantial coherence time of large scale fading coefficients, as shown in the rest of this section.

We assume the following discrete time linear system,

$$\Psi_{t+1} = \mathbf{A}\Psi_t + \zeta_t \quad (10)$$

$$\mathbf{Pr}_t = \mathbf{C}\Psi_t + \sigma_n^2 \mathbb{1} + \eta_t \quad (11)$$

where  $\mathbf{A}$  models the variation of large scale channel gains over time.  $\mathbf{A}$  is assumed to have been estimated offline in the scope of this paper. Making no assumptions on spatial correlation of large scale fading, given the high temporal correlation  $\mathbf{A}$  tends to be a diagonal matrix.  $\mathbf{C}$  is a diagonal matrix where all entries along the diagonal are the transmit powers of training symbols. The Gaussian process noise is modelled by  $\zeta$  and the measurement noise caused by erroneous location awareness and RSS measurements is modelled by a Gaussian process  $\eta$ . Corresponding covariance matrices are  $\mathbf{Q}$  and  $\mathbf{R}$ .

The problem is made more challenging by the UE being unable to perform sensing at all  $N_p$  grid points. Motivated by the work in [6] we partition the measurement vector to known and unknown parts as follows,

$$\begin{bmatrix} \mathbf{P}_{\mathbf{s}_t} - \sigma_n^2 \mathbb{1} \\ \tilde{\mathbf{P}}_{\mathbf{s}_t} - \sigma_n^2 \mathbb{1} \end{bmatrix} = \begin{bmatrix} \hat{\mathbf{C}} \\ \tilde{\mathbf{C}} \end{bmatrix} \Psi_t + \begin{bmatrix} \hat{\eta}_t \\ \tilde{\eta}_t \end{bmatrix} \quad (12)$$

where  $\mathbf{P}_{\mathbf{s}}$  is the known measurement vector from  $N_s$  active UE and  $\tilde{\mathbf{P}}_{\mathbf{s}}$  contains the unknown elements of  $\mathbf{Pr}$ . Impact of missing measurements is captured by allowing  $\tilde{\eta} \sim \mathcal{N}(0, \sigma_{\tilde{\eta}}^2)$  where  $\sigma_{\tilde{\eta}}^2 \rightarrow \infty$ . The measurement noise correlation matrix can be written as,  $\begin{bmatrix} \mathbf{R}_{11} & \mathbf{R}_{12} \\ \mathbf{R}_{21} & \mathbb{I}\sigma_{\tilde{\eta}}^2 \end{bmatrix}$

From classic KF time update and prediction equations [6],

$$\hat{\Psi}_{t|t} = E[\Psi_t | q, \mathbf{Pr}_0, \dots, \mathbf{Pr}_t] \quad (13)$$

$$\mathbf{P}_{t|t} = E[(\Psi_t - \hat{\Psi}_{t|t})(\Psi_t - \hat{\Psi}_{t|t})^T | q, \mathbf{Pr}_0, \dots, \mathbf{Pr}_t] \quad (14)$$

$$\hat{\Psi}_{t+1|t} = E[\Psi_{t+1} | q, \mathbf{Pr}_0, \dots, \mathbf{Pr}_t] \quad (15)$$

$$\mathbf{P}_{t+1|t} = E[(\Psi_{t+1} - \hat{\Psi}_{t+1|t})(\Psi_{t+1} - \hat{\Psi}_{t+1|t})^T | q, \mathbf{Pr}_0, \dots, \mathbf{Pr}_t] \quad (16)$$

where  $\hat{\Psi}$  is the estimation for  $\Psi$ . Regardless of the missing measurements, the prediction stage of the KF stays the same as it is independent from the observation process.

$$\hat{\Psi}_{t+1|t} = \mathbf{A}\hat{\Psi}_{t|t} \quad (17)$$

$$\mathbf{P}_{t+1|t} = \mathbf{A}\mathbf{P}_{t|t}\mathbf{A}^T + \mathbf{Q} \quad (18)$$

However, the time update equations now become stochastic depending on the random locations where UE perform sensing. Solutions for (15) and (16) deviate from traditional KF solutions as shown in [6],

$$\hat{\Psi}_{t|t} = \hat{\Psi}_{t|t-1} + \mathbf{K}_t(\mathbf{P}_{\mathbf{s}_t} - \sigma_n^2 \mathbb{1} - \hat{\mathbf{C}}\hat{\Psi}_{t|t-1}) \quad (19)$$

$$\mathbf{P}_{t|t} = (\mathbb{I} - \mathbf{K}_t\hat{\mathbf{C}})\mathbf{P}_{t|t-1} \quad (20)$$

where  $\mathbb{I}$  is an identity matrix and  $\mathbf{K}_t$  is the Kalman gain defined as,

$$\mathbf{K}_t = \mathbf{P}_{t|t-1}\hat{\mathbf{C}}[\hat{\mathbf{C}}\mathbf{P}_{t|t-1}\hat{\mathbf{C}}^T + \mathbf{R}_{11}]^{-1} \quad (21)$$

Hence (17), (18), (19), (20) and (21) can be used to estimate and track changes of channel gains that can be used to determine the incumbent active area as further illustrated in Section V.

## V. MAXIMUM LIKELIHOOD ESTIMATION OF INCUMBENT ACTIVE AREA

To determine the incumbent active area we adopt a similar approach to the interference temperature concept in IEEE 802.22 [7]. We are interested in estimating the contour where the RSS of the incumbent drops below a predetermined threshold. Outside this contour the SNR value of the incumbent signal is too low to be decoded by an incumbent receiver. Hence the probability of an incumbent receiver being present outside this contour is minimal and the LSA licensee is able to use the spectrum in this region.

In determining the incumbent active area we consider the following pathloss model,  $L_{ij} = K(d_0/d_{ij})^\gamma$  where  $d_{ij}$  is the distance between  $i$ th and  $j$ th reference points. Further,  $K$  and  $d_0$  are constants. We can determine the radius of contour as follows,

$$d = d_0 (PtK/\bar{P}r)^{1/\gamma} \quad (22)$$

where  $\bar{P}r$  is the predetermined RSS threshold.

From (22) the transmit power of the incumbent is proportional to the radius of contour. Given the channel estimations from Section IV we can take the maximum likelihood estimation of the transmit power as follows,

$$\hat{P}t = [(\Phi\hat{\Psi})^T \Phi\hat{\Psi}]^{-1} (\Phi\hat{\Psi})^T (\mathbf{P}_{\mathbf{s}} - \sigma_n^2 \mathbb{1}) \quad (23)$$

where  $\mathbf{P}_{\mathbf{s}}$  is the RSS of the incumbent signal measured by active UE. The value of  $Pt$  can then be used to estimate the incumbent active area contour in (22). Our approach to incumbent active area detection is summarised in Algorithm 1. Effectiveness of this approach is evaluated in Section VI.

**Algorithm 1** Light-REM construction and incumbent active area detection:  $k^{\text{th}}$  iteration

**Require:** If  $k = 1$  use the following initial conditions

- $\hat{\Psi}_{t|t-1}$  -  $N_p \times 1$  column vector of zeros
- $A$  - can be estimated offline in the scope of this paper

- 1: **if** Measurements were received from UE **then**
- 2: Calculate Kalman Gain  $\mathbf{K}_t$  from (21)
- 3: Perform measurement update in (19) and (20)
- 4: **end if**
- 5: Estimate the incumbent transmit power from (23) and the incumbent active region contour from (22)
- 6: Perform KF prediction stage by following (17) and (18)

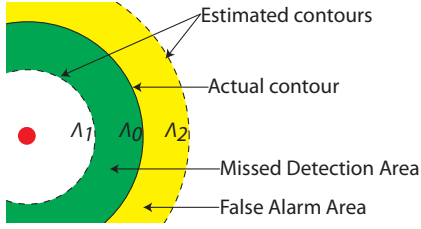


Fig. 2. Missed Detection Area (MDA) and False Alarm Area (FAA) illustration

## VI. SIMULATION AND ANALYSIS

We consider a static or slowly moving incumbent operating in 700 MHz band. The incumbent has come to an agreement with a LSA cellular operator who is allowed to use the spectrum when it is inactive. Incumbent is obliged to report to the LSA repository regarding its location, however the LSA operator should determine when the incumbent is active and take necessary steps to avoid interference. To generate RSS of the incumbent signal we use WINNER+ channel model.

We compare our light-REM based maximum likelihood estimation approach to its counterpart that does not use a light-REM in making maximum likelihood estimation. In the alternative approach we consider, the LSA licensee remembers the latest noisy channel estimation to perform maximum likelihood estimation approach. Hence, we directly compare the benefit of our KF based light-REM approach.

As the performance criteria we investigate the error in incumbent transmit power estimation, *Missed Detection Area* (MDA) and *False Alarm Area* (FAA) defined as follows,

$$\text{MDA} = (\Lambda_0 - \Lambda_1)/\Lambda_0 \quad \text{FAA} = (\Lambda_2 - \Lambda_0)/\Lambda_2 \quad (24)$$

The areas  $\Lambda_0, \Lambda_1$  and  $\Lambda_2$  are the areas as shown in Fig. 2. Our definition for MDA and FAA are analogous to Missed Detection ( $H_0|H_1$ ) and False Alarm ( $H_1|H_0$ ) in a traditional cognitive radio system ( $0 \leq \text{MDA}, \text{FAA} \leq 1$ ). From (22) we infer that  $d \propto Pt^{1/\gamma}$ . Therefore, regardless of the RSS threshold used in determining the incumbent contour we write,

$$\text{MDA} = \frac{\hat{P}t_0^{2/\gamma} - \hat{P}t_1^{2/\gamma}}{\hat{P}t_0^{2/\gamma}} \quad \text{FAA} = \frac{\hat{P}t_2^{2/\gamma} - \hat{P}t_0^{2/\gamma}}{\hat{P}t_2^{2/\gamma}} \quad (25)$$

TABLE I  
SIMULATION PARAMETERS

| Parameter        | Value  |
|------------------|--|
| Grid size        | 9 x 9 (80 x 80 m)  |
| Incumbent power  | $Pt = 10$ dBm  |
| KF linear model  | $A = \mathbb{I}, C = Pt(mW) \times \mathbb{I}$   |
| Noise covariance | $Q = \text{var}(\zeta) \times \mathbb{I}, R = \text{var}(\eta) \times \mathbb{I}$                                    |
| Noise model      | $\eta \sim \mathcal{N}(0, 1e-12), \zeta \sim \mathcal{N}(0, 1e-16),$<br>$n \circ n^* \sim \mathcal{N}(1e-11, 1e-22)$ |

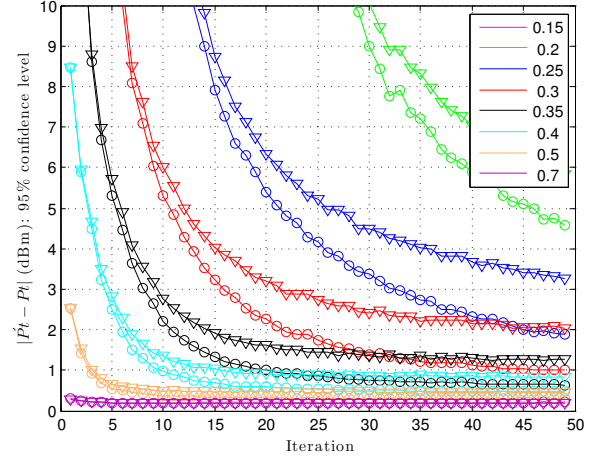


Fig. 3. Difference between the estimated and actual incumbent power in dBm, 95% confidence level is shown. We compare our light-REM approach (marker: circle) with the alternative maximum likelihood approach that does not use light-REM (marker: triangle). Value of  $q$  is shown in the legend. Note:  $q = 0.15$  results in a highly erroneous estimation.

We vary  $q$ , the probability of a UE taking part in light-REM construction, and determine how fast our algorithm converges to the solution. The variable  $q$  is directly proportional to the traffic overhead, hence a smaller value is desirable. However, the lower traffic overhead comes at a price as illustrated in the rest of the section. Some relevant parameters used in simulations are shown in Table I.

### A. Incumbent Power Detection

In Fig. 3 we compare the difference between estimated and actual incumbent transmit power. This stochastic variable is represented by its 95% confidence level, which is a better representation than mean and/or variance. Simulations were run for 50 iterations considering 100,000 independent scenarios.

Fig. 3 shows that both approaches eventually converge to a steady state error level determined by  $q$ . Although error is low when  $q \geq 0.5$ , due to high overhead this region is less feasible. When  $q \leq 0.2$  the overhead is low, however the error is  $> 10$  dBm even after 25 iterations.

When  $0.2 < q < 0.5$ , which is a more reasonable operating region for the system, our approach has a clear edge over the alternative. For instance, when  $q = 0.35$  our approach guarantees the error in incumbent power estimation is less than 2 dBm after 11 iterations with 95% confidence. Whereas the alternative guarantees the same after 15 iterations. When  $q = 0.3$  those figures are 22 and 45 respectively.

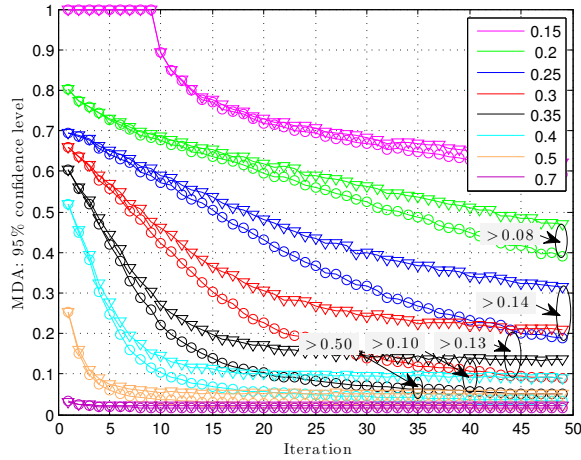


Fig. 4. Missed Detection Area as defined in (24), the 95% confidence level.

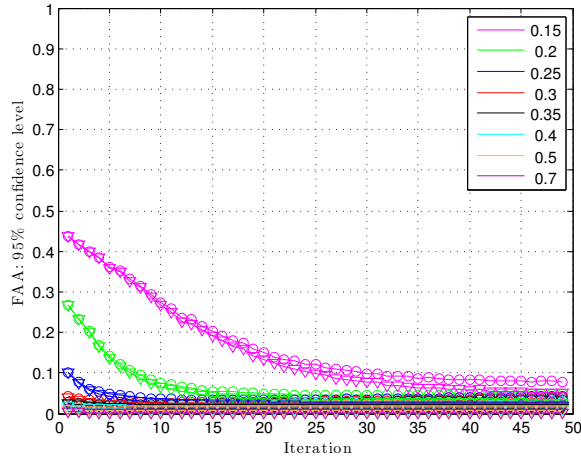


Fig. 5. False Alarm Area as defined in (24), the 95% confidence level.

### B. Missed Detection Area

Fig. 4 shows how the 95% confidence level of MDA varies through 50 iterations. We have the incumbent constantly active at one randomly selected reference point and we determine the MDA using (24). Similar to Fig. 3 all curves appear to eventually reach a steady state MDA level depending on the UE density. The difference of steady state MDA when  $q = 0.4$  is in the order of 0.05. When  $q = 0.25, 0.30$  the difference is expected to be  $> 0.13$ . As we get close to  $q \leq 0.2$  region the gain is reduced. This MDA performance improvement in the typical operational region of  $q$  justifies the use of our KF based light-REM approach.

Also, it should be noted that  $q = 0.15$  curve is constant at  $MDA = 1$  for the first 9 iterations. We infer that the incumbent is not detected in the first 9 iterations with 95% probability.

### C. False Alarm Area

Fig. 5 shows how the 95% confidence level of FAA varies through 50 iterations. Clearly  $q = 0.15$  stands out with a high FAA rate in comparison to other curves. This is due to lack of availability of measurements for any approach to

be effective. For all  $q > 0.2$  values the FAA falls below 0.05 after about 7 iterations. Both approaches appear to be highly effective in reducing the FAA. Since the difference between two approaches is marginal, statistical inference is that both approaches are indifferent in regard to FAA.

Since FAA converges to steady state faster than MDA, one could marginally increase the estimated incumbent power  $\hat{P}_t$  to improve the MDA at the expense of worsened FAA. However, that is considered to be beyond the scope of this paper.

## VII. CONCLUSION

In this paper we proposed an extension to the existing LSA cellular operator architecture by incorporating the concept of light-REM. Our approach is based on running a discrete time Kalman Filter to construct and track changes to light-REM, then taking maximum likelihood estimation for the incumbent user active region. We consider a challenging situation where geo-localised spectrum measurements used in the system are highly distorted and the majority of the measurements is missing. We compare the proposed approach to the nearest comparable alternative of taking maximum likelihood estimation that does not use a light-REM. Simulation results show that our approach is more effective than its counterpart when spectrum measurements are taken when the UE density is within the range  $0.20 < q < 0.50$ , which is a realistic region of operation for the system.

## ACKNOWLEDGMENT

This work has been supported by Intel's University Research Office.

## REFERENCES

- [1] European Telecommunications Standards Institute (ETSI), "Electromagnetic compatibility and radio spectrum matters (ERM); mobile broadband services in the 2300 mhz 2400 mhz frequency band under licensed shared access regime - system reference document," Tech. Rep.
- [2] B. A. Jayawickrama, E. Dutkiewicz, I. Oppermann, M. D. Mueck, and G. Fang, "Downlink power allocation algorithm for licence-exempt LTE systems using kriging and compressive sensing based spectrum cartography," in *Globecom 2013 - Wireless Communications Symposium (GC13 WC)*, Atlanta, USA, Dec. 2013.
- [3] B. A. Jayawickrama, E. Dutkiewicz, I. Oppermann, G. Fang, and J. Ding, "Improved performance of spectrum cartography based on compressive sensing in cognitive radio networks," in *IEEE ICC 2013 - Wireless Communications Symposium (ICC'13 WCS)*, Budapest, Hungary, Jun. 2013.
- [4] R. Mahapatra and E. Strinati, "Interference-aware dynamic spectrum access in cognitive radio network," in *Personal Indoor and Mobile Radio Communications (PIMRC), 2011 IEEE 22nd International Symposium on*, sept. 2011, pp. 396–400.
- [5] B. Sayrac, A. Galindo-Serrano, S. B. Jemaa, J. Riihijarvi, and P. Mhnen, "Bayesian spatial interpolation as an emerging cognitive radio application for coverage analysis in cellular networks," *Transactions on Emerging Telecommunications Technologies*, vol. 24, no. 7-8, pp. 636–648, 2013. [Online]. Available: <http://dx.doi.org/10.1002/ett.2724>
- [6] X. Liu and A. Goldsmith, "Kalman filtering with partial observation losses," in *Decision and Control, 2004. CDC. 43rd IEEE Conference on*, vol. 4, Dec 2004, pp. 4180–4186 Vol.4.
- [7] "IEEE Standard for Information technology– Local and metropolitan area networks– Specific requirements– Part 22: Cognitive Wireless RAN Medium Access Control (MAC) and Physical Layer (PHY) specifications: Policies and procedures for operation in the TV Bands," *IEEE Std 802.22-2011*, pp. 1–680, 2011.